EARLY STAGE EXPERIMENT
Science Description

Investigator(s): Rob Rogers, Jon Zawislak (Co-PIs), Ghassan Alaka, Jason Dunion, Heather Holbach, Trey Alvey (U. Utah), Josh Wadler (U. Miami/RSMAS) (Co-Is)

Requirements: TD, TS, Category 1

Science Objectives:

1) Collect datasets that can be used to improve the understanding of intensity change processes, as well as the initialization and evaluation of 3-D numerical models, particularly for TCs experiencing moderate vertical wind shear [*IFEX Goals 1, 3*]

2) Obtain a quantitative description of the kinematic and thermodynamic structure and evolution of intense convective systems (convective bursts) and the nearby environment to examine their role in TC intensity change [*IFEX Goals 1, 3*]

3) Improve our understanding of the physical processes responsible for the formation and evolution of arc clouds, as well as their impacts on TC structure and intensity in the short-term [*IFEX Goals 1, 3*]

Description of Science Objectives:

SCIENCE OBJECTIVE #1: *Collect datasets that can be used to improve the understanding of intensity change processes, as well as the initialization and evaluation of 3-D numerical models, particularly for TCs experiencing moderate vertical wind shear*
<u>[Analysis of Intensity Change Processes Experiment, AIPEX]</u>

Motivation: While some improvements in operational tropical cyclone (TC) intensity forecasting have been made in recent years (DeMaria et al. 2014), predicting changes in TC intensity (as defined by the 1-min. maximum sustained wind) remains problematic. In particular, the operational prediction of rapid intensification (RI) has proven to be especially difficult (Kaplan et al. 2010). The significant impact of such episodes has prompted the Tropical Prediction Center/National Hurricane Center (TPC/NHC) to declare it as its top forecast priority (Rappaport et al. 2009).

Processes that govern TC intensification span spatial and temporal scales from the environmental to vortex to convective and smaller scales. Recent work has focused on the precipitation distribution and structure to assess regimes associated with TC intensification. Studies using airborne Doppler radar (Rogers et al. 2013) and passive microwave satellite (e.g., Alvey et. al 2015; Tao and Jiang 2015) observations have compared the inner-core structure of intensifying and non-intensifying TCs. Precipitation and deep convection in intensifying cases were found to be more symmetrically distributed and located preferentially inside the radius of maximum wind (RMW) compared to non-intensifying cases. Predictability of the azimuthal and radial distribution of precipitation and deep convection within TCs, however, remains low.

Thus, identifying and understanding the environmental and internal (within the inner core) mechanisms that govern the azimuthal and radial distribution of precipitation and deep convection could improve the understanding of the intensification process. Recent studies indicate that these mechanisms may include: the interaction of the vortex with environmental vertical wind shear and dry air, vortex-scale subsidence, surface enthalpy fluxes from the underlying ocean, and precipitation mode (i.e., shallow, moderately deep, and deep convection, as well as stratiform rain).

The goal of this experiment is to collect datasets that can be used to: 1) improve the initialization and evaluation of 3-D numerical models; 2) improve the understanding of intensity change processes across multiple scales, with particular focus on the mechanisms that govern the azimuthal and radial distribution of precipitation and deep convection. TCs that are experiencing moderate vertical wind shear (5–10 m s^{-1}) over a deep layer (850–200 hPa) are of particular interest, since this range of shear values is often associated with considerable uncertainty with respect to the prospect for TC intensification (Bhatia and Nolan 2013). The overarching goal is to improve the ability to predict the timing and magnitude of intensification, particularly RI, events.

Background: Prior studies have found a number of large-scale environmental factors that are generally favorable for TC intensification, including low environmental vertical wind shear, high ocean heat content, and elevated low- to mid-tropospheric humidity. Thus far, statistically-based prediction schemes that employ predictors derived from large-scale environmental fields and GOES infrared satellite imagery have generally been shown to provide the most skillful objective RI guidance (Kaplan et al. 2015). These schemes include the SHIPS rapid intensification index (SHIPS-RII) (Kaplan et al. 2010) and the more recently developed Bayesian and logistic regression RI models (Rozoff and Kossin 2011). Kaplan et al. (2015) showed that these statistical models are capable of explaining roughly 20% of the skill of Atlantic basin RI forecasts at a lead-time of 24 h. The remaining 80% of the skill not explained by the statistical models is assumed to be attributable either to processes not explicitly accounted for by those models or by limitations in the predictability of RI events.

On the vortex-scale, a number of observational studies have found that intensifying TCs have more precipitation and convective bursts occur within the high inertial stability region inside the RMW (e.g., Rogers et al. 2013, 2015, 2016). This configuration is favorable for TC intensification for two hypothesized reasons: 1) in the high inertial stability region, heat energy is much more efficiently converted to kinetic energy (Schubert and Hack 1982; Vigh and Schubert 2009), and 2) diabatic heating within the high inertial stability region enables angular momentum surfaces to be drawn inward at the RMW, resulting in tangential wind spinup (Smith and Montgomery 2016).

Observational studies have also found that intensifying TCs typically have more symmetrically distributed precipitation and deep convection than non-intensifying TCs (e.g., Rogers et al. 2013; Alvey et al. 2015; Tao and Jiang 2015). This is consistent with idealized modeling studies that show that TC intensification is most sensitive to the axisymmetric, azimuthal wavenumber-0 component of diabatic heating (e.g., Nolan et al. 2007). One principal environmental factor that can prevent the development of this symmetry is vertical wind shear. The interaction of TCs with environmental vertical wind shear typically results in a wavenumber-1 asymmetry in vertical motion and precipitation, in which upward vertical motion and deep convection is favored in the downshear semicircle, while downward motion and suppression of deep convection is observed in the upshear semicircle (e.g., Marks et al. 1992; Reasor et al. 2013; Rogers et al. 2016; Zawislak et al. 2016). An increase in asymmetry can lead to the decrease in the projection of diabatic heating onto the axisymmetric, azimuthal wavenumber-0 component that has been shown to be important for TC intensification. However, the magnitude of this asymmetry can exhibit considerable variability, particularly within the moderate shear regime (5–10 m s^{-1}) that has been shown to be problematic for operational intensity forecasts (Bhatia and Nolan 2013). This suggests the importance of understanding what governs the azimuthal distribution of precipitation and deep convection.

Recent studies have used airborne Doppler radar and dropsonde data to examine what hinders the development of precipitation symmetry in sheared TCs (Rogers et al. 2016; Zawislak et al. 2016; Nguyen et al. 2017). These studies show evidence for several potential hindering factors. First, convective downdrafts associated with the downshear convection can cool and stabilize the lower troposphere in the left of shear and upshear quadrants. Second, subsidence in the upshear quadrants can increase the temperature and decrease the relative humidity of the mid-troposphere, effectively capping the lower troposphere. Third, dry air can be transported laterally from the environment into the TC's upshear quadrants. These hindering factors could be mitigated through several potential mechanisms, as listed in the hypotheses below.

Hypotheses: The following hypotheses will guide the sampling strategies for TCs that have the potential to undergo (rapid) intensification:

1. Intensification is favored when precipitation and deep convection are distributed symmetrically and located preferentially inside the radius of maximum wind (RMW).
2. The local kinematic (e.g., location and depth of radial inflow, vertical alignment of the vortex) and thermodynamic forcing (e.g., SST, available moisture, and RH) are key in governing whether precipitation (deep convection) is symmetrically distributed and primarily inside the RMW.
3. Symmetry is favored when: (a) the mid-troposphere is moistened upshear due to detrainment from mid-tropospheric congestus, evaporation of falling stratiform rain, or reduced lateral advection of dry air from the environment; (b) the lower troposphere is convectively unstable in the upshear quadrants due to enhanced surface enthalpy fluxes from the underlying ocean and/or reduced convective downdrafts.

EARLY STAGE EXPERIMENT
Science Description

Aircraft Pattern/Module Descriptions: Missions will be targeted for systems that have a reasonable chance of undergoing intensification based on statistical and numerical model forecast guidance. When possible (i.e., subject to range, timing, and other logistical constraints), missions will begin at least 24 h prior to the expected onset of intensification, while the TC is still at tropical depression or tropical storm intensity. This enables the documentation of TC structure during the time leading up to intensification onset (if it indeed occurs). Ideally missions will continue every 12 h, as long as feasible. If either the P-3 or G-IV aircraft cannot fly every 12 h the experiment can still be conducted provided that the gap between missions for any one of the two aircraft does not exceed 24 h. Although all intensification rates are of interest, priority will be given to those with a high potential for RI according to model guidance and/or are forecast to experience at least moderate (5–10 m s^{-1}) vertical wind shear over a deep layer. There are a few possible configurations for the execution of this experiment, as outlined below:

1. Both P-3 and G-IV are available
P-3 Pattern #1: AIPEX
G-IV Pattern #1: AIPEX
G-IV Pattern #2: AIPEX

This is the optimal configuration for this experiment as, under this scenario, the P-3 and G-IV would coordinate operations (i.e., takeoff times would allow both aircraft to sample the TC simultaneously). The P-3 will sample the inner-core with the standard rotated Figure-4 pattern (*P-3 Pattern #1: AIPEX*), while the G-IV will sample the outer environment and near-TC environment (typically around 60 n mi, or 100 km) with either the circumnavigation (*G-IV Pattern #1: AIPEX*) or star (*G-IV Pattern #2: AIPEX*) pattern.

2. Only P-3 is available
P-3 Pattern #1: AIPEX
P-3 Pattern #2: AIPEX

When the G-IV is not available for coordinated operations, either because of operational tasking requirements or aircraft unavailability, P-3 targeted observations in the near environment and inner core can still contribute towards the objectives of the experiment. In this scenario there are two possible strategies for sampling, which depend on whether the precipitation distribution is asymmetric:

(a) TC is highly asymmetric:

This option will be chosen when the precipitation distribution in the targeted TC is expected to be highly asymmetric during the mission. Such an asymmetric configuration would allow for a high-altitude P-3 circumnavigation pattern to at least target the precipitation-free upshear semicircle, and when hazard avoidance is possible the downshear quadrants. Indications of an appropriate magnitude of asymmetry may include:

1) Visible, infrared, or microwave satellite imagery indicates an exposed or partially exposed low-level circulation center (Fig. ES-1).
2) The environmental vertical wind shear, as indicated by SHIPS, is expected to be sufficient (> 5 m s^{-1}) during the mission to result in an asymmetric precipitation structure.
3) High-resolution numerical guidance (i.e. HWRF) forecast a lack of precipitation in the upshear semicircle of the TC during the mission.

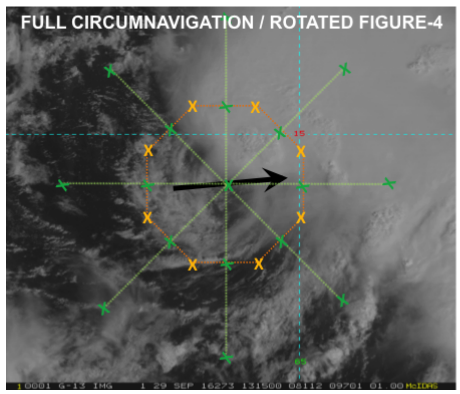

Figure ES-1. *Figure-4 in green, circumnavigation in orange, shear vector in black, 'X' is a dropsonde location*

Given this scenario, the P-3 will sample the near environment and inner core with a pattern that includes a high-altitude circumnavigation and, optimally, a rotated Figure-4 (*P-3 Pattern #2: AIPEX*). If time doesn't permit for a complete rotated Figure-4, then a single Figure-4 can be substituted (Fig. ES-1). The radius of the circumnavigation should be as close to the inner-core precipitation shield as safety allows, as best determined through available visible or infrared satellite, microwave, or radar imagery. The high-altitude circumnavigation allows for increased azimuthal and vertical dropsonde data coverage, particularly in the critical, precipitation-free upshear region that may fill in as intensification commences.

(b) TC is relatively symmetric:

This scenario applies to a targeted TC that has the potential for intensification, but the precipitation is expected to be too symmetric during the mission for the P-3 high-altitude circumnavigation to be conducted safely. Here, the P-3 will sample the inner-core vortex structure with the standard rotated Figure-4 pattern (*P-3 Pattern #1: AIPEX*).

3. Only G-IV is available:

G-IV Pattern #1: AIPEX

G-IV Pattern #2: AIPEX

This option is less preferable as targeted observations of the vortex structure are also important towards the objectives of the experiment. This option applies to any targeted TC that has the potential for intensification, regardless of asymmetric structure. Under this option, the G-IV will sample the outer and near environments with either the circumnavigation (*G-IV Pattern #1: AIPEX*) or star (*G-IV Pattern #2: AIPEX*), and requires that hazard avoidance permit the G-IV to obtain measurements within/very near the inner core.

4. Additional modules

If the opportunity arises during the execution of AIPEX, fly the Convective Burst and Evolution Module (CBM) or Arc Cloud Module (Arc Cloud) (see accompanying discussion for Science Objectives #2 and #3 of this experiment). The CBM would be optimal for determining the structure and evolution of deep convection within the framework of the broader vortex-scale circulation as it interacts with vertical shear (if appropriate), while the Arc Cloud module would be ideal for documenting locations within the vortex circulation encountering significant low-to mid-level dry air and determining the impact of the associated outflow boundaries on the boundary layer temperature and moisture distribution.

Analysis Strategy: The general analysis strategy follows that performed in recent observational studies (Reasor et al. 2013; Zhang et al. 2013; Rogers et al. 2016; Zawislak et al. 2016; Nguyen et al. 2017). The analysis strategy includes assessing and documenting the time evolution of the following:

- *Azimuthal and radial distribution of inner-core precipitation and deep convection* (P-3 TDR/LF, possibly G-IV TDR). The inner-core precipitation asymmetry, and its projection onto the axisymmetric, azimuthal wavenumber-0 component will be assessed quantitatively (assuming sufficient azimuthal coverage). The location of precipitation and convective bursts relative to the RMW will be examined.

- *Precipitation mode, particularly upshear* (P-3 TDR/LF, possibly G-IV TDR). An analysis of the precipitation mode (shallow, moderately deep, deep convection, as well as stratiform rain), using the vertical velocity and reflectivity structure, will allow for an assessment as to whether moistening of the inner core occurs through upscale growth of convection (moistening from convective detrainment at gradually higher altitudes), or from the top-down via stratiform rain as hydrometeors produced downshear are transported azimuthally upshear.

- *Low-wavenumber thermodynamic and kinematic structure of the boundary layer* (P-3/G-IV dropsondes, DWL for kinematic only). The thermodynamic focus will be on the boundary layer cooling by convective downdrafts and the subsequent recovery via surface enthalpy fluxes from the underlying ocean in the downstream (upshear-left through downshear-right) quadrants. Surface enthalpy fluxes will be calculated where dropsondes are paired with AXBTs that provide sea surface temperature. The kinematic focus will be on obtaining measurements of the strength and depth of boundary layer inflow and convergence in the boundary layer, both in a symmetric sense and relative to the shear vector (when relevant). Additionally, the gradient and agradient flow in the boundary layer will be calculated.

- *Low-wavenumber thermodynamic and kinematic structure above the boundary layer* (P-3/G-IV dropsondes, P-3/G-IV TDR and DWL for kinematic only). The presence of mid-tropospheric dry air is of particular interest. Assuming mid-tropospheric dry air is present (most likely in the upshear quadrants), the potential sources of this dry air (vortex-scale subsidence or lateral advection from the environment) and how this upshear dry air is removed (i.e., through detrainment from congestus or evaporation of stratiform precipitation) will be assessed.

- *Vortex tilt* (P-3 TDR, possibly G-IV TDR). Assuming sufficient TDR coverage, the vortex tilt will be examined quantitatively by merging TDR analyses from each Figure-4. If the vortex tilt appears to decrease rapidly during a flight, individual TDR analyses can be used to qualitatively examine the time evolution of vortex tilt during the alignment process.

- *Vertical wind shear and upper-level divergence* (G-IV dropsondes). These quantities will be computed and compared with global model analyses. The vertical distribution of shear will also be evaluated, as upper-level shear is hypothesized to be less deleterious than low-level shear.

The overarching hypothesis is that, by performing the above analyses for multiple AIPEX data sets collected during both RI and non-RI events, it will be possible to determine the conditions that are triggers for RI. This analysis strategy can also assist in the evaluation of 3-D numerical models, including the sufficiency (or lack thereof) of the horizontal resolution, and the microphysical and planetary boundary layer parameterization schemes.

References:

Alvey, G.R. III, J. Zawislak, and E. Zipser, 2015: Precipitation Properties Observed during Tropical Cyclone Intensity Change. *Mon. Wea. Rev.*, **143**, 4476–4492. doi: 10.1175/MWR-D-15-0065.1.

Bhatia, K. T., and D. S. Nolan, 2013: Relating the skill of tropical cyclone intensity forecasts to the synoptic environment. *Wea. Forecasting*, **28**, 961–980, doi: 10.1175/WAF-D-12-00110.1.

DeMaria, M., C. R. Sampson, J. A. Knaff, and K. D. Musgrave, 2014: Is tropical cyclone intensity guidance improving? *Bull. Amer. Meteor. Soc.*, **95**, 387–398, doi:10.1175/BAMS-D-12-00240.1.

Kaplan, J., M. DeMaria, and J. A. Knaff, 2010: A revised tropical cyclone rapid intensification index for the Atlantic and eastern North Pacific basins. *Wea. Forecasting*, **25**, 220–241, doi: 10.1175/2009WAF2222280.1.

Kaplan, J., and Coauthors, 2015: Evaluating environmental impacts on tropical cyclone rapid intensification predictability utilizing statistical models. *Wea. Forecasting*, **30**, 1374–1396, doi: 10.1175/WAF-D-15-0032.1.

Marks, F. D., Jr., R. A. Houze Jr., and J. F. Gamache, 1992: Dual-aircraft investigation of the inner core of Hurricane Norbert. Part I: Kinematic structure. *J. Atmos. Sci.*, **49**, 919–942, doi: 10.1175/1520-0469(1992)049<0919:DAIOTI>2.0.CO;2.

Nguyen, L. T., R. Rogers, and P. Reasor 2017: Thermodynamic and kinematic influences on precipitation symmetry in sheared tropical cyclones: Bertha and Cristobal (2014). *Mon. Wea. Rev.* In review.

Nolan, D. S., Y. Moon, and D. P. Stern, 2007: Tropical cyclone intensification from asymmetric convection: Energetics and efficiency. *J. Atmos. Sci.*, **64**, 3377–3405, doi: 10.1175/JAS3988.1.

Rappaport, E. N., and Coauthors, 2009: Advances and Challenges at the National Hurricane Center. *Wea. Forecasting*, **24**, 395–419.

Reasor, P. D., R. F. Rogers, and S. Lorsolo, 2013: Environmental flow impacts on tropical cyclone structure diagnosed from airborne Doppler radar composites. *Mon. Wea. Rev.*, **141**, 2949–2969, doi: 10.1175/MWR-D-12-00334.1.

Rogers, R., P. Reasor, and S. Lorsolo, 2013: Airborne Doppler observations of the inner-core structural differences between intensifying and steady-state tropical cyclones. *Mon. Wea. Rev.*, **141**, 2970–2991, doi: 10.1175/MWR-D-12-00357.1.

Rogers, R. F., P. D. Reasor, and J. A. Zhang, 2015: Multiscale structure and evolution of Hurricane Earl (2010) during rapid intensification. *Mon. Wea. Rev.*, **143**, 536–562, doi: 10.1175/MWR-D-14-00175.1.

Rogers, R., J. Zhang, J. Zawislak, H. Jiang, G. Alvey, E. Zipser, and S. Stevenson, 2016: Observations of the structure and evolution of Hurricane Edouard (2014) during intensity change. Part II: Kinematic structure and the distribution of deep convection. *Mon. Wea. Rev.*, **144**, 3355–3376, doi: 10.1175/MWR-D-16-0017.1.

Rozoff, C. M., and J. P. Kossin, 2011: New probabilistic forecast models for the prediction of tropical cyclone rapid intensification. *Wea. Forecasting*, **26**, 677–689, doi: 10.1175/WAF-D-10-05059.1.

Schubert, W. H., and J. J. Hack, 1982: Inertial stability and tropical cyclone development. *J. Atmos. Sci.*, **39**, 1687–1697, doi: 10.1175/1520-0469(1982)039<1687:ISATCD>2.0.CO;2.

Tao, C., and H. Jiang, 2015: Distributions of shallow to very deep precipitation–convection in rapidly intensifying tropical cyclones. *J. Climate*, **28**, 8791–8824, doi: 10.1175/JCLI-D-14-00448.1.

Vigh, J. L., and W. H. Schubert, 2009: Rapid development of the tropical cyclone warm core. *J. Atmos. Sci.*, **66**, 3335–3350, doi: 10.1175/2009JAS3092.1.

Zawislak, J., H. Jiang, G. Alvey, E. Zipser, R. Rogers, J. Zhang, and S. Stevenson, 2016: Observations of the structure and evolution of Hurricane Edouard (2014) during intensity change. Part I: Relationship between the thermodynamic structure and precipitation. *Mon. Wea. Rev.*, **144**, 3333–3354, doi: 10.1175/MWR-D-16-0017.1.

Zhang, J. A., R. F. Rogers, P. Reasor, E. Uhlhorn, and F. D. Marks Jr., 2013: Asymmetric hurricane boundary layer structure from dropsonde composites in relation to the environmental wind shear. *Mon. Wea. Rev.*, **141**, 3968–3984, doi: 10.1175/MWR-D-12-00335.1.

EARLY STAGE EXPERIMENT
Science Description

SCIENCE OBJECTIVE #2: *Obtain a quantitative description of the kinematic and thermodynamic structure and evolution of intense convective systems (convective bursts) and the nearby environment to examine their role in TC intensity change*
[Convective Burst Structure and Evolution Module, CBM]

Motivation: The objectives are to obtain a quantitative description of the kinematic and thermodynamic structure and evolution of intense convective systems (convective bursts) and the nearby environment to examine their role in TC intensity change.

Background: It has long been known that deep convection is an integral component of TC structure. What has received greater attention in recent years is the potential role that deep convection, termed here "convective bursts", or CBs, representing the peak updrafts and highest echo tops, plays in TC evolution, in particular intensity evolution. Various hypotheses attribute their contribution to TC intensification by vortex gradient adjustment to the imposed diabatic heating in the high-inertial stability region inside the RMW (e.g., Shapiro and Willoughby 1982, Schubert and Hack 1982, Hack and Schubert 1986, Nolan and Grasso 2003, Nolan et al. 2007, Vigh and Schubert 2009, Pendergrass and Willoughby 2009, Rogers et al. 2013, 2015, 2016), convergence of angular momentum surfaces in the lower troposphere and boundary layer (Smith and Montgomery 2016), upper-level subsidence warming around the CB periphery (e.g., Heymsfield et al. 2001, Guimond et al. 2010, Rogers 2010, Zhang and Chen 2012, Chen and Zhang 2013, Chen and Gopal 2015), stretching and axisymmetrization in vortical hot towers (Hendricks et al. 2004, Montgomery et al. 2006, Reasor et al. 2009), and vortex alignment/downshear reformation (Reasor et al. 2009, Molinari and Vollaro 2010, Nguyen and Molinari 2012, Reasor and Eastin 2012, Stevenson et el. 2014, Rogers et al. 2015, Nguyen and Molinari 2015). While these studies have emphasized the role of deep convection in TC intensification, other studies have focused on the role of shallow to moderate convection, and even stratiform precipitation, in initiating TC intensification (Kieper and Jiang 2012, Zagrodnik and Jiang 2014, Tao and Jiang 2015, Tao et al. 2017, Nguyen et al. 2017). Common to these and other (e.g., Miyamoto and Takemi 2015) studies, though, is that TC intensification is favored when precipitation, including CBs, are preferentially located inside the RMW with a maximum azimuthal distribution.

Vertical shear is one factor that has been shown to be important in organizing precipitation, including CBs, azimuthally around the TC vortex. This has generally been attributed to the fact that vertical shear tilts the vortex, leading to preferred regions of vortex-scale low-level convergence and upward motion downshear and low-level divergence and subsidence upshear (Jones 1995, Bender 1997, Frank and Ritchie 2001, Black et al. 2002, Corbosiero and Molinari 2003, Rogers et al. 2003, Braun et al. 2006, Wu et al. 2006, Reasor et al. 2009, Reasor and Eastin 2012, Reasor et al. 2013, Dolling and Barnes 2014, DeHart et al. 2014). Recent composite studies of vortices in shear using airborne Doppler radar have shown that the shear-induced circulations are maximized downshear right (DSR) (low-level convergence/upward motion) and upshear left (USL) (low-level divergence/downward motion) (Reasor et al. 2013, DeHart et al.

2014). A similar composite methodology has been performed in a CB-relative coordinate system (Wadler et al. 2017). This study found that the peak updraft magnitude and altitude for CBs was minimized DSR, consistent with the notion that this is the quadrant where CBs are initiated. Peak updraft magnitude and altitude increase in the DSL quadrant, as the CBs mature, and they reach their highest and strongest values USL. A similar shear-relative azimuthal relationship was found for echo top height. Significantly, when stratifying TCs by intensity change, it was found that the most significant differences in CB structure between intensifying and non-intensifying TCs were located in the USL quadrant. Intensifying TCs have CBs with stronger peak updrafts, at a higher altitude, with higher echo tops in the USL quadrant than non-intensifying TCs. This relationship suggests that the structure and evolution of CBs, which are to some extent a function of the local environment from which they initiate downshear and mature upshear — including convective available potential energy, midlevel humidity, and subsidence upshear (Zawislak et al. 2016, Rogers et al. 2016, Nguyen et al. 2017) — is an important factor to consider in assessing the potential for a TC to intensify.

It should be noted that the above descriptions presume that CBs do translate downwind, i.e., upshear. However, in some situations, mostly revealed from modeling studies (Munsell et al. 2017, Chen et al. 2017), CBs can remain "trapped" on the downshear side. In fact, cases where the CBs remain downshear were more likely to be associated with non-intensifying periods of TC evolution. This is consistent with the notion of greater azimuthal symmetry of diabatic heating being associated with TC intensification. CBs propagating into the upshear quadrants may also be related to a greater likelihood of vortex alignment, as revealed in the observational analysis of Hurricane Earl (2010; Rogers et al. 2015) and a WRF-ARW ensemble forecast of Edouard (2014; Munsell et al. 2017).

The results described above are valid for composites of many different CBs from many different TCs. They therefore lack the temporal continuity needed to measure the structure of specific individual (or groups of) CBs, and how they evolve in a shear-relative sense. The purpose of this module is to repeatedly sample individual (or groups of) CBs to provide this temporal continuity.

Hypotheses: The following hypotheses will guide the sampling strategies for CBs. One set of hypotheses is for CBs that translate downwind/upshear, the other set is for CBs that remain confined downshear:

1. CBs are preferentially initiated in the DSR quadrant; as such, the updraft maxima is likely to be weaker and at a lower altitude in this quadrant;

For CBs translating downwind/upshear:

2. Traveling downwind into the DSL quadrant, peak updrafts will strengthen and be located at a higher altitude;

3. The strength of the CB in the USL quadrant (as measured by strength and height of peak updraft and echo top height relative to the DSL quadrant) will vary depending on the local, vortex-scale environment of the convection. This environment includes midlevel humidity, strength of subsidence upshear, and sea surface temperature (and CAPE) on the downshear side of the TC;
4. If the CB strength USL is higher (lower) than DSL, the TC will intensify (not intensify).

For CBs remaining confined downshear:

5. The structural evolution will follow a similar path to those CBs translating downwind/upshear; i.e., updraft peaks beginning in lower to middle troposphere, then ascending with time before becoming dominated by downdrafts and collapse while remaining downshear
6. TC will not intensify

Aircraft Pattern/Module Descriptions:

P-3 Module #1: CBM

This is a stand-alone module that takes 1–2 h to complete. Execution is dependent on system attributes, aircraft fuel and weight restrictions, and proximity to operations base. It can be flown separately within a mission designed to study local areas of convection or at the end of one of the survey patterns. Once a local area of intense convection is identified, the P-3 will transit at altitude (10–12 kft) to the nearest point just outside of the convective cores and sample the convective area. The sampling pattern will be a series of inbound/outbound radial penetrations or bowtie patterns (when sampling a CB near the RMW of a tropical storm or hurricane). If the CB is at or near the RMW, repeated sampling can allow for a following of the burst around the storm. This is especially useful to sample the structural evolution of the burst as it moves around the storm. If the CB remains confined to the downshear side of the TC rather than translate upshear, the pattern should still be flown.

Analysis Strategy: Radar analyses will be performed for each radial pass through the CB, preferentially with a temporal spacing of 30 minutes or less. These analyses will provide high-frequency observations of the structure of the CB, as measured by the peak updraft magnitude and altitude and echo top heights. Additionally, the full spectrum of vertical velocity associated with each radar analysis will be evaluated using contoured frequency by altitude diagrams (CFADs; Yuter and Houze 1995) to obtain a more complete picture of the updraft and downdraft structure and evolution of the CB. Ideally a CB will be flown beginning with its initiation (likely to be downshear) and then followed around the storm as it travels through the downwind quadrants and into the upshear quadrants (or continuously sampled on the downshear side if it remains confined there). Dropsondes released at the starting and ending points of each radial leg will document the thermodynamic structure of the boundary layer radially bracketing the CB. Optimally, the G-IV will be flying in the storm to provide deep-layer humidity profiles around the storm in addition to the P-3 dropsondes. If the G-IV is not available, the module could still be flown to examine the evolution using the Doppler radar and boundary layer thermodynamics from the P-3 dropsondes.

In addition to the observational analysis described above, the high-resolution data collected in this module is planned to be embedded within the typical Hurricane Ensemble Data Assimilation System (HEDAS; e.g., Aksoy et al. 2013) framework to carry out storm-scale data assimilation that focuses specifically on the high-resolution analysis of the identified intense convective region. With current technology, a smaller domain with 1-km grid spacing will be nested within the HEDAS 3-km analysis domain, where the data will be assimilated for the duration of its collection (1–2 hours, at 5–10 min intervals). This is a typical setup that has been traditionally used in continental storm-scale radar data assimilation applications and has been shown to be effective to obtain realistic storm structures in analyses and short-range forecasts. With such high-resolution analyses, we hope to be able to obtain fully three-dimensional model representations of the observed convective regions for more detailed investigation, as well as investigate their short-range predictability. In an observing system experiment (OSE) mode, various assimilation experiments can also be devised to investigate hypothetical scenarios for how an observed convective region could interact with the surrounding vortex and impact its evolution.

References:

Aksoy, A., S. D. Aberson, T. Vukicevic, K. J. Sellwood, S. Lorsolo, and X. Zhang (2013), Assimilation of high-resolution tropical cyclone observations with an ensemble Kalman filter using NOAA/AOML/HRD's HEDAS: Evaluation of the 2008–11 vortex-scale analyses, *Mon. Wea. Rev.*, **141**, 1842–1865, doi: http://dx.doi.org/10.1175/MWR-D-12-00194.1.

Bender, M. A., 1997: The effect of relative flow on the asymmetric structure in the interior of hurricanes. *J. Atmos. Sci.*, **54**, 703–724, doi:10.1175/1520-0469(1997)054<0703:TEORFO>2.0.CO;2.

Black, M. L., J. F. Gamache, F. D. Marks, C. E. Samsury, and H. E. Willoughby, 2002: Eastern Pacific Hurricanes Jimena of 1991 and Olivia of 1994: The effect of vertical shear on structure and intensity. *Mon. Wea. Rev.*, **130**, 2291–2312, doi:10.1175/1520-0493(2002)130<2291:EPHJOA>2.0.CO;2.

Braun, S. A., M. T. Montgomery, and Z. Pu, 2006: High-resolution simulation of Hurricane Bonnie (1998). Part I: The organization of eyewall vertical motion. *J. Atmos. Sci.*, **63**, 19–42, doi:10.1175/JAS3598.1.

Chen, H., and S. G. Gopalakrishnan, 2015: A study on the asymmetric rapid intensification of Hurricane Earl (2010) using the HWRF system. *J. Atmos. Sci*., **72**, 531–550, doi:10.1175/JAS-D-14-0097.1.

Chen, H., and D. L. Zhang, 2013: On the rapid intensification of Hurricane Wilma (2005). Part II: Convective bursts and the upper-level warm core. *J. Atmos. Sci*., **70**, 146–162, doi:10.1175/JAS-D-12-062.1.

Chen, H., S.Gopalakrishnan, J.A. Zhang, R.F. Rogers, Z. Zhang, and V. Tallapragada, 2017: Use of HWRF ensembles for providing improved understanding of hurricane RI problem: Case study of Hurricane Edouard (2014). *J. Atmos. Sci*., in review.

Corbosiero, K. L., and J. Molinari, 2003: The relationship between storm motion, vertical wind shear, and convective asymmetries in tropical cyclones. *J. Atmos. Sci*., **60**, 366–376, doi:10.1175/1520-0469(2003)060<0366:TRBSMV>2.0.CO;2.

DeHart, J. C., R. A. Houze Jr., and R. F. Rogers, 2014: Quadrant distribution of tropical cyclone inner-core kinematics in relation to environmental shear. *J. Atmos. Sci*., **71**, 2713–2732, doi:10.1175/JAS-D-13-0298.1.

Dolling, K., and G. M. Barnes, 2014: The evolution of Hurricane Humberto (2001). *J. Atmos. Sci*., **71**, 1276–1291, doi:10.1175/JAS-D-13-0164.1.

Frank, W. M., and E. A. Ritchie, 2001: Effects of vertical wind shear on the intensity and structure of numerically simulated hurricanes. *Mon. Wea. Rev*., **129**, 2249–2269, doi:10.1175/1520-0493(2001)129<2249:EOVWSO>2.0.CO;2.

Guimond, S. R., G. M. Heymsfield, and F. J. Turk, 2010: Multiscale observations of Hurricane Dennis (2005): The effects of hot towers on rapid intensification. *J. Atmos. Sci*., **67**, 633–654, doi:10.1175/2009JAS3119.1.

Hack, J. J., and W. H. Schubert, 1986: Nonlinear response of atmospheric vortices to heating by organized cumulus convection. *J. Atmos. Sci*., **43**, 1559–1573, doi:10.1175/1520-0469(1986)043<1559:NROAVT>2.0.CO;2.

Hendricks, E. A., M. T. Montgomery, and C. A. Davis, 2004: The role of "vortical" hot towers in the formation of Tropical Cyclone Diana (1984). *J. Atmos. Sci*., **61**, 1209–1232, doi:10.1175/1520-0469(2004)061<1209:TROVHT>2.0.CO;2.

Heymsfield, G. M., J. B. Halverson, J. Simpson, L. Tian, and T. P. Bui, 2001: ER-2 Doppler radar investigations of the eyewall of Hurricane Bonnie during the Convection and Moisture Experiment-3. *J. Appl. Meteor*., **40**, 1310–1330, doi:10.1175/1520-0450(2001)040<1310:EDRIOT>2.0.CO;2.

Jones, S. C., 1995: The evolution of vortices in vertical shear. I: Initially barotropic vortices. *Quart. J. Roy. Meteor. Soc*., **121**, 821–851, doi:10.1002/qj.49712152406.

Kieper, M. E., and H. Jiang, 2012: Predicting tropical cyclone rapid intensification using the 37 GHz ring pattern identified from passive microwave measurements. *Geophys. Res. Lett*., **39**, L13804, doi:10.1029/2012GL052115.

Miyamoto, Y., and T. Takemi, 2015: A triggering mechanism for rapid intensification of tropical cyclones. *J. Atmos. Sci*., **72**, 2666–2681, doi:10.1175/JAS-D-14-0193.1.

Molinari, J., and D. Vollaro, 2010: Rapid intensification of a sheared tropical storm. *Mon. Wea. Rev*., **138**, 3869–3885, doi:10.1175/2010MWR3378.1.

Montgomery, M. T., M. Nicholls, T. Cram, and A. Saunders, 2006: A “vortical” hot tower route to tropical cyclogenesis. *J. Atmos. Sci*., **63**, 355–386, doi:10.1175/JAS3604.1.

Munsell, E.B., F. Zhang, J.A. Sippel, S.A. Braun, and Y. Weng, 2017: Dynamics and Predictability of the Intensification of Hurricane Edouard (2014). *J. Atmos. Sci*., **74**, 573–595, doi: 10.1175/JAS-D-16-0018.1.

Nguyen, L. T., and J. Molinari, 2012: Rapid intensification of a sheared, fast-moving hurricane over the Gulf Stream. *Mon. Wea. Rev*., **140**, 3361–3378, doi:10.1175/MWR-D-11-00293.1.

Nguyen, L. T., and J. Molinari, 2015: Simulation of the downshear reformation of a tropical cyclone. *J. Atmos. Sci*., **72**, 4529–4551, doi:10.1175/JAS-D-15-0036.1.

Nguyen, L.T., R.F. Rogers, and P.D. Reasor, 2017: Thermodynamic and kinematic influences on precipitation symmetry in sheared tropical cyclones: Bertha and Cristobal (2014). *Mon. Wea. Rev*., in review.

Nolan, D. S., and L. D. Grasso, 2003: Nonhydrostatic, three-dimensional perturbations to balanced, hurricane-like vortices. Part II: Symmetric response and nonlinear simulations. *J. Atmos. Sci*., **60**, 2717–2745, doi:10.1175/1520-0469(2003)060<2717:NTPTBH>2.0.CO;2.

Nolan, D. S., Y. Moon, and D. P. Stern, 2007: Tropical cyclone intensification from asymmetric convection: Energetics and efficiency. *J. Atmos. Sci*., **64**, 3377–3405, doi:10.1175/JAS3988.1.

Pendergrass, A. G., and H. E. Willoughby, 2009: Diabatically induced secondary flows in tropical cyclones. Part I: Quasi-steady forcing. *Mon. Wea. Rev*., **137**, 805–821, doi:10.1175/2008MWR2657.1.

Reasor, P. D., and M. D. Eastin, 2012: Rapidly intensifying Hurricane Guillermo (1997). Part II: Resilience in shear. *Mon. Wea. Rev*., **140**, 425–444, doi:10.1175/MWR-D-11-00080.1.

Reasor, P. D., M. D. Eastin, and J. F. Gamache, 2009: Rapidly intensifying Hurricane Guillermo (1997). Part I: Low-wavenumber structure and evolution. *Mon. Wea. Rev*., **137**, 603–631, doi:10.1175/2008MWR2487.1.

Reasor, P. D., R. F. Rogers, and S. Lorsolo, 2013: Environmental flow impacts on tropical cyclone structure diagnosed from airborne Doppler radar composites. *Mon. Wea. Rev*., **141**, 2949–2969, doi:10.1175/MWR-D-12-00334.1.

Rogers, R.F., 2010: Convective-scale structure and evolution during a high-resolution simulation of tropical cyclone rapid intensification. *J. Atmos. Sci*., **67**, 44–70, doi:10.1175/2009JAS3122.1.

Rogers, R., S. S. Chen, J. E. Tenerelli, and H. E. Willoughby, 2003: A numerical study of the impact of vertical shear on the distribution of rainfall in Hurricane Bonnie (1998). *Mon. Wea. Rev*., **131**, 1577–1599, doi:10.1175//2546.1.

Rogers, R., P. D. Reasor, and S. Lorsolo, 2013: Airborne Doppler observations of the inner-core structural differences between intensifying and steady-state tropical cyclones. *Mon. Wea. Rev*., **141**, 2970–2991, doi:10.1175/MWR-D-12-00357.1.

Rogers, R., P. D. Reasor, and J. A. Zhang, 2015: Multiscale structure and evolution of Hurricane Earl (2010) during rapid intensification. *Mon. Wea. Rev*., **143**, 536–562, doi:10.1175/MWR-D-14-00175.1.

Rogers, R.F., J.A. Zhang, J. Zawislak, H. Jiang, G.R. Alvey III, E.J. Zipser, and S.N. Stevenson, 2016: Observations of the structure and evolution of Hurricane Edouard (2014) during intensity change. Part II: Kinematic structure and the distribution of deep convection. *Mon. Wea. Rev*., **144**, 3355-3376.

Schubert, W. H., and J. J. Hack, 1982: Inertial stability and tropical cyclone development. *J. Atmos. Sci*., **39**, 1687–1697, doi:10.1175/1520-0469(1982)039<1687:ISATCD>2.0.CO;2.

Shapiro, L. J., and H. E. Willoughby, 1982: The response of balanced hurricanes to local sources of heat and momentum. *J. Atmos. Sci*., **39**, 378–394, doi:10.1175/1520-0469(1982)039<0378:TROBHT>2.0.CO;2.

Smith, R. K., and M. T. Montgomery, 2016: The efficiency of diabatic heating and tropical cyclone intensification. *Quart. J. Roy. Meteor. Soc*., **142**, 2081–2086, doi:10.1002/qj.2804.

Stevenson, S. N., K. L. Corbosiero, and J. Molinari, 2014: The convective evolution and rapid intensification of Hurricane Earl (2010). *Mon. Wea. Rev.*, **142**, 4364–4380, doi:10.1175/MWR-D-14-00078.1.

Tao, C., and H. Jiang, 2015: Distributions of shallow to very deep precipitation–convection in rapidly intensifying tropical cyclones. *J. Climate*, **28**, 8791–8824, doi:10.1175/JCLI-D-14-00448.1.

Tao, C., H. Jiang, and J. Zawislak, 2017: The Relative Importance of Stratiform and Convective Rainfall in Rapidly Intensifying Tropical Cyclones. *Mon. Wea. Rev.*, **145**, 795–809, doi: 10.1175/MWR-D-16-0316.1.

Vigh, J. L., and W. H. Schubert, 2009: Rapid development of the tropical cyclone warm core. *J. Atmos. Sci.*, **66**, 3335–3350, doi:10.1175/2009JAS3092.1.

Wadler, J., R.F. Rogers, and P.D. Reasor, 2017: Radial and azimuthal variations in convective burst structure in tropical cyclones from airborne Doppler observations. *Mon. Wea. Rev.*, manuscript in review.

Wu, L., S. A. Braun, J. Halverson, and G. Heymsfield, 2006: A numerical study of Hurricane Erin (2001). Part I: Model verification and storm evolution. *J. Atmos. Sci.*, **63**, 65–86, doi:10.1175/JAS3597.1.

Zagrodnik, J. P., and H. Jiang, 2014: Rainfall, convection, and latent heating distributions in rapidly intensifying tropical cyclones. *J. Atmos. Sci.*, **71**, 2789–2809, doi:10.1175/JAS-D-13-0314.1.

Zawislak, J., H. Jiang, G. R. Alvey III, E. J. Zipser, R. F. Rogers, J. A. Zhang, and S. N. Stevenson, 2016: Observations of the structure and evolution of Hurricane Edouard (2014) during intensity change. Part I: Relationship between the thermodynamic structure and precipitation. *Mon. Wea. Rev.*, **144**, 3333–3354, doi:10.1175/MWR-D-16-0018.1.

Zhang, D.-L., and H. Chen, 2012: Importance of the upper level warm core in the rapid intensification of a tropical cyclone. *Geophys. Res. Lett.*, **39**, L02806, doi:10.1029/2012GL052355.

Yuter, S. E., and R. A. Houze, 1995: Three-dimensional kinematic and microphysical evolution of Florida cumulonimbus. Part II: Frequency distributions of vertical velocity, reflectivity, and differential reflectivity. *Mon. Wea. Rev.*, **123**, 1941–1963, doi:10.1175/1520-0493(1995)123<1941:TDKAME>2.0.CO;2.

EARLY STAGE EXPERIMENT
Science Description

SCIENCE OBJECTIVE #3: *Improve our understanding of the physical processes responsible for the formation and evolution of arc clouds, as well as their impacts on TC structure and intensity in the short-term* (Arc Cloud Module)

Motivation: Arc clouds are common features in mid-latitude thunderstorms and mesoscale convective systems. They often denote the presence of a density current that forms when dry mid-level (~600–850 hPa) air has interacted with precipitation. The convectively-driven downdrafts that result reach the surface/near-surface and spread out from the convective core of the thunderstorm. Substantial arc clouds (i.e. > 55 n mi (100 km) in length and lasting for several hours) are also common features in the tropics (Fig. ES-2), particularly on the periphery of African easterly waves (AEWs) and TCs. However, the physical processes responsible for such tropical arc clouds as well as their impacts on the short-term evolution of their parent disturbances are not well understood.

Background: Large low-level thunderstorm outflow boundaries emanating from TCs have been previously documented and have been hypothesized to occur when high vertical wind shear promotes the intrusion of dry mid-level air toward the TC eyewall (Knaff and Weaver 2000). However, the mid-level moisture found in the *moist tropical* North Atlantic sounding described by Dunion (2011) is hypothesized to be insufficiently dry to generate extensive near-surface density currents around an AEW or TC. However, Dunion (2011) also described two additional air masses that are frequently found in the tropical North Atlantic and Caribbean during the summer months and could effectively initiate the formation of large arc clouds: (1) the Saharan Air Layer (*SAL*) and (2) *mid-latitude dry air intrusions*. Both of these air masses were found to contain substantially dry air (~50% less moisture than the *moist tropical* sounding) in the mid-levels that could support convectively-driven downdrafts and large density currents. Furthermore, outward-propagating arc clouds on the periphery of AEWs or TCs could be enhanced by near-surface super-gradient winds induced by the downward transport of high momentum air. Since most developing tropical disturbances in the North Atlantic are associated with a mid-level jet and/or mesoscale convective vortex near a state of gradient balance, any convectively-driven downdrafts would inject high momentum air into a near-surface environment that often contains a weaker horizontal pressure gradient. In such cases, density currents may be temporarily enhanced during local adjustments to gradient balance. Finally, tropical arc clouds may be further enhanced by outward-propagating diurnal pulses that originate from the convective core of the tropical disturbance (see TC Diurnal Cycle objective in the Mature Stage Experiment). New GOES IR TC diurnal cycle imagery indicates that arc clouds tend to form along the leading edge of outwardly propagating diurnal pulses that are associated with the TC diurnal cycle. The diurnal pulses reach peripheral radii where low to mid-level dry air is often located (e.g. R=300–500 km) at remarkably predictable times of day (e.g. 400 km at ~1200–1500 LST). Therefore, UW-CIMSS real-time TC diurnal cycle and visible satellite imagery, as well as P-3 LF radar data (where TC diurnal pulses are denoted by 25+ dBZ semi-circular convective bands propagating away from the storm) will be used to monitor the diurnal pulse propagation throughout the local morning hours and signs of arc cloud formation.

As arc clouds propagate away from the tropical disturbance, they visibly emerge from underneath the central dense overcast that can obscure them from visible an infrared satellite view. Therefore, when arc clouds are identified using satellites, they are often in the middle to later stages of their lifecycles. Hence, the mechanism of enhanced low-level outflow is likely occurring at the time of satellite identification, while the mechanism of cooling/drying of the boundary layer has already occurred (though the effects may still be observable by aircraft flight-level, GPS dropsonde, and satellite data). This necessitates that the arc clouds be identified and sampled as early in their lifecycle as possible using available aircraft observations (e.g. flight-level, GPS dropsonde and P-3 LF radar, and P-3/G-IV Doppler radar data) and satellite imagery (e.g. TC diurnal cycle infrared, visible, infrared, and microwave).

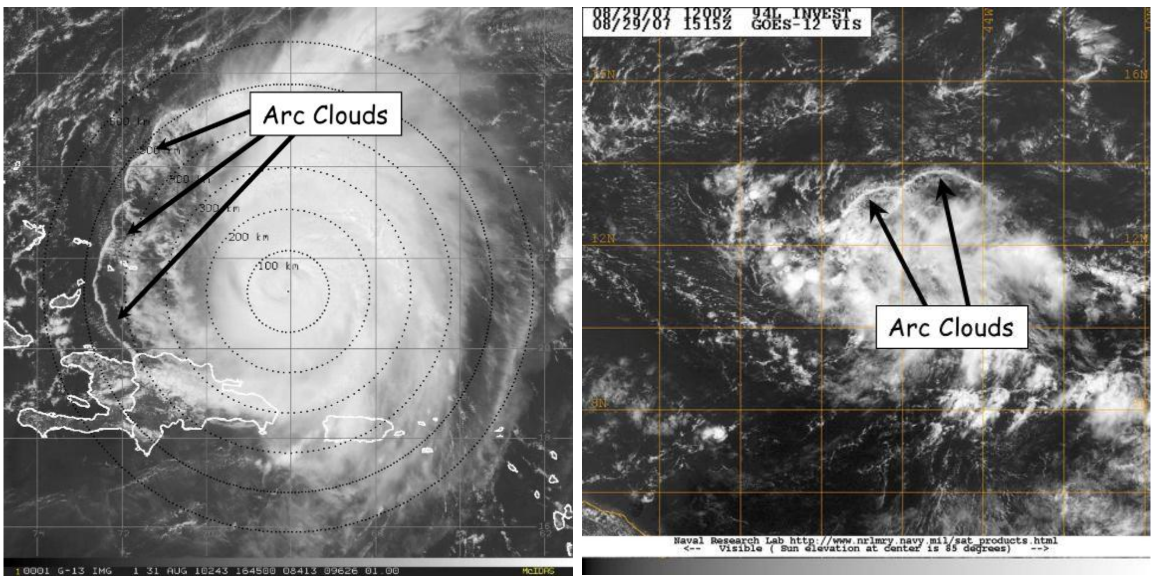

Figure ES-2: *GOES visible satellite imagery showing arc clouds racing away from the convective cores of (left) 2003 Hurricane Isabel and (right) 2007 Pre-Tropical Depression Felix.*

Hypotheses: Arc clouds form along the leading edge of TC diurnal pulses, are particularly favored to occur at R~105–215 n mi (~200–400 km) in areas with mid-level (~600–800 hPa) dry air (≤45 mm total precipitable water [TPW]), and can act to temporarily stabilize the TC environment.

EARLY STAGE EXPERIMENT
Science Description

Aircraft Pattern/Module Descriptions:

P-3 Module #1: Arc Cloud
G-IV Module #1: Arc Cloud

> When arc clouds emanating from the periphery of the TC convective core are identified using satellite imagery and/or P-3 LF radar, perform this break-away pattern by transecting orthogonally across to these outwardly propagating features.

Analysis Strategy: This experiment seeks to collect observations across arc cloud features in the periphery of mature TCs using aircraft flight-level, GPS dropsonde, and TDR data to improve our understanding of the physical processes responsible for their formation and evolution, as well as how these features may affect TC structure and intensity in the short-term. Flight-level and GPS dropsonde data will be used to calculate changes in static stability and possible impacts on surface fluxes both ahead of and behind the arc cloud (e.g. enhanced stability/reduced surface fluxes behind the arc cloud leading edge). TDR data will be used to define the vertical structure of the kinematics ahead of, across and behind the arc cloud. Finally, kinematics and thermodynamics associated with arc cloud events will be compared to corresponding locations in model analysis fields (e.g. GFS and HWRF).

References:

Dunion, J.P., 2011: Rewriting the climatology of the tropical North Atlantic and Caribbean Sea atmosphere. *J. Climate,* **24***,* 893–908.

Knaff, J.A., and J.F. Weaver, 2010: A mesoscale low-level thunderstorm outflow boundary associated with Hurricane Luis. *Mon. Wea. Rev.,* **128***,* 3352–3355.